

Hastaneye Yatırılan COVID-19 Hastalarında Akciğer Bilgisayarlı Tomografi Parankimal Bulguları ile C Reaktif Protein Arasındaki İlişki

The Relationship Between Parenchymal Findings of Chest Computed Tomography and C Reactive Protein in COVID-19 Patients at Hospital Admission

Derya Deniz Altıntaş, Ayhan Şenol

Gazi Yaşargil Eğitim ve Araştırma Hastanesi, Radyoloji Bölümü, Diyarbakır, Türkiye

Cite as: Derya Deniz Altıntaş, Ayhan Şenol COVID19 hastalarında nodül ve CRP Kocaeli Med J 2021;10(2):160-166.

Öz

GİRİŞ ve AMAÇ: Bu çalışmada, hastaneye yatışta Toraks Bilgisayarlı Tomografide (BT) COVID-19 pnömonisine ait parankimal bulguların C reaktif protein (CRP) ile ilişkisini araştırmayı amaçladık.

YÖNTEM ve GEREÇLER: 1 Nisan-30 Mayıs 2020 tarihleri arasında akciğer tomografisinde akciğer bulguları saptanan ve hastaneye başvuran ardışık 192 COVID-19 hastası çalışmaya dahil edildi. COVID-19 pulmoner bulguları başvuru Toraks BT ile değerlendirildi

BULGULAR: 192 hastanın ortanca yaşı 44 (31-59) yıl olup, bunların %46,8'i (90) kadındı. Medyan CRP değeri 15.2mg/L (2.0-55) olarak bulundu. Hastaların Toraks BT bulguları şöyledi: %69.2 (133) buzlu cam opaklığı, %33.8 (65) konsolidasyon, %6.2 (12) ters halo, %11.9 (23) çılgın kaldırım, %20.8 (40) ayrı nodül, %5.7 (11) pulmoner vasküler genişleme, %3.6 (7) bronşektazi ve %17.1 (33) fibrozis ile. Nodül prezentasyonu olmayan hastalarda ortalama CRP 42,8±59,1 nodül prezentasyonu olan hastalarda ise 34,7±53,2 bulundu. CRP ile ilgili bağımsız öngörücüleri belirlemek için; Yukarıda açıklanan göğüs BT parametreleri lineer regresyonda değerlendirildi. Göğüs BT'sinde nodül varlığı (-26.1CI %95; (-49.0,-3.1), p = 0.026), Bsti-CT skoru (20,6, CI %95; 7,6, 33,6, p) arasında istatistiksel olarak anlamlı ilişki saptandı. = 0,002) ve CRP değerleri.

TARTIŞMA ve SONUÇ: Çalışmamızda, hastaneye başvuran semptomatik COVID-19 hastalarında nodül gibi atipik bulguları olan hastaların Toraks BT'sinde tipik bulguları olanlara göre CRP düzeylerinin daha düşük olduğunu bulduk.

Anahtar Kelimeler: c reaktif protein, COVID-19, göğüs bilgisayarlı tomografi, nodül

Geliş tarihi / Received:

04.06.2021

Kabul tarihi / Accepted:

20.08.2021

Sorumlu Yazar/Corresponding Author:

Derya Deniz Altıntaş Gazi Yaşargil Eğitim ve Araştırma Hastanesi, Radyoloji Bölümü, Diyarbakır, Türkiye

deryadenizaltintas@gmail.com

ORCID: 0000-0002-2618-9177

A. Şenol 0000-0001-5467-0307

Abstract

INTRODUCTION: In this study, we aimed to investigate the relationship between the parenchymal findings of COVID-19 pneumonia on chest Computed Tomography (CT) and C reactive protein (CRP) at hospital admission.

METHODS: 192 consecutive COVID-19 patients with pulmonary findings on chest CT, who were admitted to the hospital between 1st April to 30th May 2020, were included in the study. COVID-19 pulmonary findings were evaluated in admission chest CT

RESULTS: Median age of 192 patients was 44 (31-59) years and 46.8% (90) of them were female. Median CRP value was found to be 15.2mg/L (2.0-55). Chest CT findings of the patients were as follows: 69.2% (133) with ground glass opacity, 33.8% (65) with consolidation, 6.2% (12) with reversed halo, 11.9% (23) with crazy-paving, 20.8% (40) with discrete nodules, 5.7% (11) with pulmonary vascular enlargement, 3.6% (7) with bronchiectasis and 17.1% (33) with fibrosis. The mean CRP was found to be 42.8±59.1 in patients without nodule presentation and 34.7±53.2 in patients with nodule presentation. In order to determine independent predictors related to CRP; chest CT parameters described above were assessed in the linear regression. Association with statistical significance were determined between the presence of nodule on chest CT (-26.1CI 95%; (-49.0,-3.1), p = 0.026), Bsti-CT score (20.6, CI 95%; 7.6, 33.6, p= 0.002) and CRP values.

DISCUSSION AND CONCLUSION: In our study, we found that patients with atypical findings as nodules had lower CRP levels than those with typical findings on chest CT in symptomatic COVID-19 patients admitted to the hospital.

Keywords: c reactive protein, chest computed tomography, COVID-19, nodula



INTRODUCTION

At the end of 2019, SARS-CoV-2 disease (COVID-19) due to severe acute respiratory syndrome coronavirus 2 (SARS-CoV-2) was identified for the first time in Wuhan, a city in the Hubei Province of China, as a cause of the disease resulting in pneumonia, and it was defined as pandemic disease by the World Health Organization (1-3). COVID-19 may manifest as a mild upper respiratory tract infection or as a lower respiratory tract infection with symptoms ranging from acute respiratory distress syndrome to severe pneumonia in symptomatic patients. Alternative rapid diagnostic methods have been needed because the PCR test, the gold standard for the diagnosis of SARS-CoV-2, takes a long time to get a result and the sensitivity of PCR is between 60 to 70% depending on the viral load in the upper respiratory tract and swabbing quality (4,5).

The unexpected, extremely high admission rates of symptomatic patients in suspect of COVID-19 pneumonia to emergency departments forced the diagnosis of COVID-19 pneumonia to be done radiologically to isolate the patients at early stage and to hospitalize the patients as soon as possible (6). Chest computed tomography (CT) is used as an expeditious and effective diagnostic imaging modality in diagnosis of COVID-19 pneumonia, given that it has very characteristic CT presentations such as ground glass opacity (GGO), consolidation and crazy paving (7,8) Also, CT imaging along with presence of blood inflammation markers plays a major role in the management and clinical follow-up of COVID-19 pneumonia. CT sensitivity and specificity reported in various COVID-19 Studies have been found to differ significantly among symptomatic patients (60% to 98% and 25% to 53%, respectively. (9-11). However, chest CT alone may not be sufficient to diagnose symptomatic patients with uncharacteristic chest CT findings and the diagnosis should be supported by inflammation markers such as C-reactive protein (CRP).

In this study, we aimed to investigate the relationship between hospital admission COVID-19 chest CT findings and CRP value among patients with COVID-19

MATERIAL AND METHOD

Study design

This is a single-center, retrospective and observational study. 205 consecutive patients, who were admitted to the hospital between 1st to 30th April 2020 with the diagnosis of PCR (+) Covid-19 and with pulmonary involvement on chest CT, were included in the study. Patients with known structural lung disease, lung cancer chronic obstructive pulmonary disease, rheumatologic disease and active non-COVID infection were excluded from the study. Patients without COVID-19 pulmonary findings were excluded from the study. Also, the patients whose diagnosis were not confirmed by repeated PCR test in-hospital course were not included in the study. The demographic and clinical characteristics of the patients were obtained from hospital database. Hemogram, CRP and other biochemical measurements were repeated according to the need during the hospital course in addition to the measurements at admission.

Chest CT protocol

The CT scans were obtained with a General Electric Optima 540 (GE Healthcare Systems, Chicago, Illinois, USA) Using the following parameters: 120 kVp, 100 mA, 1.5 mm collimation, 1.375:1 pitch, reconstruction matrix of 512 x 512, slice thickness of 1.25 mm, and lung kernel algorithm. The CT protocol were performed in a supine position during breath-holding at full inspiration. All CT images were evaluated using a lung window, with a window level of -500 HU and window width of 1500 HU.

Chest CT image analysis

Two experienced radiologists in thorax CT radiology evaluated the thin-section CT images respectively and make a decision in consensus. Parenchymal findings were defined as typical, indeterminate, atypical and non-covid according to the Radiological Society of North America (RSNA) consensus statement. The groups defined as typical, indeterminate and atypical were also evaluated as mild, moderate and severe involvement according to the Computed tomography (CT) weighted scoring according to the British Society of Thoracic Imaging (BSTI) consensus statement. The distribution of pulmonary lesions also were defined central (predominantly lung hilum, involving mainly the central two-third of the lung), peripheral (predominantly subpleural, involving mainly the peripheral one-third of the lung), and bronchocentric, as depending on their location in the lung. The predominant patterns were reported on CT images as ground glass opacity (GGO, hazy areas of increased attenuation without obscuration of the underlying vessels), consolidation (homogeneous opacification of the parenchyma with obscuration of the underlying vessels), reversed halo, crazy-paving (GGO with inter lobular and intralobular septal thickening), discrete nodule, pulmonary vascular enlargement and fibrosis. On the CT images, other atypical pulmonary findings such as air bronchogram, cavitation, bronchiectasia, pleural effusion, pericardial effusion, pneumothorax and mediastinal lymphadenopathy (defined as a lymphnode greater than 1 cm in short-axis diameter) were also defined.

This study was approved by the Institutional Ethics Board of the Ministry of Health and our hospital. The study protocol conforms to the Declaration of Helsinki (12).

Statistical analysis

All statistical analyses were performed using the IBM SPSS software (IBM SPSS Statistics for Windows, Version 24.0, IBM Corp. Armonk, N.Y.) Continuous variables are presented as mean \pm Standard deviations (SD), or if non-normal distribution given as median interquartilerange 25–75% (IQR). Categorical variables were expressed as percentages. Correlation between variables was performed using Spearman's rank or Pearson correlation test. Linear regression model was used to assess correlates of CRP level and Thoracic CT findings. In all the statistical analyses, a p value of < 0.05 is considered statistically significant.

RESULTS

For the study, 205 patients were evaluated. Of them, 13 (6.3%) patients were excluded from the study due to absence of any pulmonary findings in chest CT. Finally, 192 patients were included in the study. Median age of 192 patients included in the study was 44 (31-59) years and 46.8% (90) of them were female. Median CRP value at the admission value was found to be 15.2mg/L (2.0-55). Involvement rates of the lungs were as follows: 26.5% (51) with the right lung, 22.9% (44) with the left lung, 50.5% (97) with bilateral involvement. According to RSNA classification, 50.5% (97), 26.5% (51), 17.7% (34) and 5.2% (10) of the patients were classified as typical, indeterminate, atypical and non-covid respectively. As per BSTI-CT weight scoring; frequencies of mild, moderate and severe diseases among the patients were 23.6% (43), 32.4% (59) and 45.0% (80) respectively. 15.1% (29), 3.6% (7), 30.2% (58) 51.0% (98) of the patients had as upper lobe, middle lobe, lower lobe and diffuse involvement, respectively. Lesions distribution in the lung were found to be centrally in 8.8% (17), peripheral in 65.1% (125) and bronchocentric in 26.0% (50) of the patients. Chest CT findings of the patients were as follows: 69.2% (133) with GGO, 33.8% (65) with consolidation, 6.2% (12) with reversed halo, 11.9% (23) with crazy-paving, 20.8% (40) with discrete nodula, 5.7% (11) with pulmonary vascular enlargement, 3.6% (7) with bronchiectasis and 17.1% (33) with fibrosis. In order to determine independent predictors related to CRP; chest CT parameters described above were assessed in the linear regression. Association with statistical significance were determined between the presence of nodule on chest CT (-26.1 CI 95%; (-49.0,-3.1), $p = 0.026$), BSTI-CT score (20.6, CI 95%; 7.6, 33.6, $p = 0.002$) and CRP values at admission (Table 1). Also, the relationship between BSTI-CT score and CRP was shown in boxplot analysis (Figure 1). The mean CRP was found to be 42.8 ± 59.1 in patients without nodule presentation and 34.7 ± 53.2 in patients with nodule presentation (Figure 2). The Area Under Curve (AUC) value for CRP and absence of nodule presentation on chest CT was determined as 0.62 (95% CI 0.53-0.70, $p = 0.02$) using ROC analysis (Figure 3).

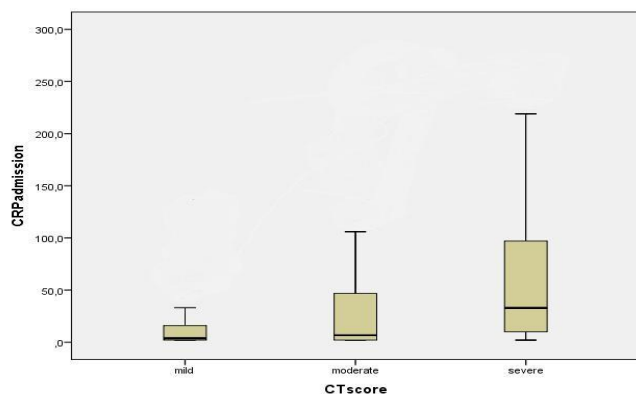


Figure 1. Boxplot analysis of the relationship between BSTI-CT score and CRP. BSTI; British society of thoracic imaging, CT; computed tomography

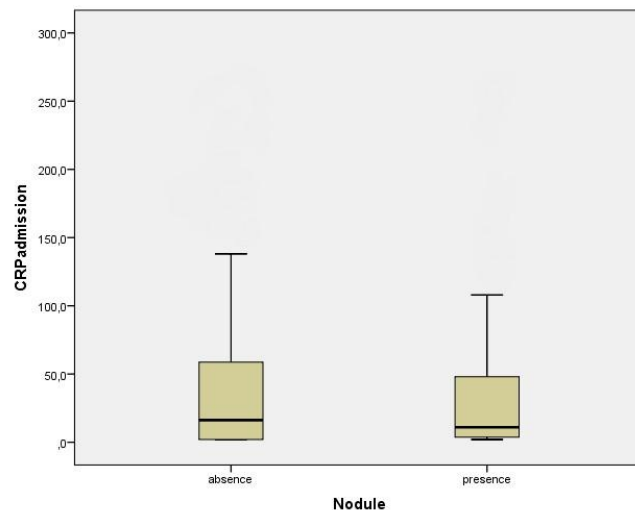


Figure 2. Boxplot analysis of relationship between chest CT presentation with/without nodula and CRP. CRP; C-reactive protein, CT; computed tomography

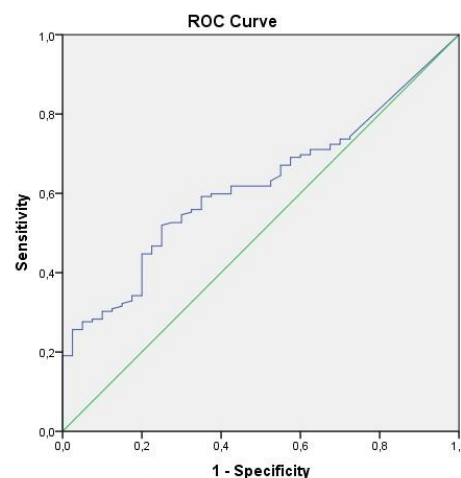


Figure 3. ROC graphics to detect the AUC value of admission CRP for absence of nodula presentation. AUC; areac under curve, CRP; C-reactive protein, ROC; receiver operating characteristic

Table 1. Multivariable linear regression analysis between CRP and COVID-19 chest CT pulmonary findings

Variables	Regression Coefficients %95 CI	p value
Unilateral vs Bilateral	-2.2 (-36.9, 49.9)	0.81
BSTI-CT score (mild/moderate/severe)	20.6 (7.6, 33.6)	0.002
Distribution of pulmonary lesions (central/peripheral/bronchocentric)	-3.0 (-34.9, 29.0)	0.69
GGO	-7.6 (-25.7, 10.5)	0.41
Consolidation	9.3 (-9.3, 28.1)	0.32
Reverse-halo	15.8 (-22.5, 54.3)	0.41
Crazy paving	15.5 (-14.4, 45.5)	0.30
Nodula	-26.1 (-49.0, -3.1)	0.026
Pulmonary vascular enlargement	4.3 (-34.5, 43.3)	0.82
Bronchiectasia	10.6 (-35.9, 57.2)	0.65
Fibrosis	11.9 (-10.2, 34.1)	0.29

BSTI, british society of thoracic imaging; CRP, C-reactive protein; CT, computed tomography; GGO, ground glass opacity

DISCUSSION

The most common reason of admission to the hospital is pneumonia among the patients with COVID-19. Between 15% and 30% of hospitalized patients develop acute respiratory distress syndrome (ARDS), the main cause of death in COVID-19 (13). Bilateral, subpleural, peripheral GGO, consolidation, reverse halo and crazy paving are the common chest CT parenchymal findings in hospitalized and symptomatic COVID-19 patients (14). Pulmonary findings of COVID-19 pneumonia have been classified in the report published by RSNA as a consensus statement in the last year (15). In this report, COVID-19 CT imaging findings are divided into 4 groups as follows: typical appearance, indeterminate appearance, atypical appearance and negative for pneumonia. Typical appearance is defined by the presence of specific distribution of focal or multifocal GGO with or without consolidation, crazy paving, reverse halo sign findings. Indeterminate appearance is defined as multifocal, diffuse, perihilar or unilateral GGO or few very small GGO with or without consolidation lacking a specific distribution and are nonrounded or nonperipheral. In the atypical appearance group, there are findings such as isolated lobar or segmental consolidation with or without GGO, discrete small nodules, lung cavitation and smooth interlobular septal thickening. A similar classification was published by BSTI in 2020. Classic and probable patterns in the classification of the BSTI report overlap with the findings in the RSNA typical and indeterminate appearance of COVID-19 classifications (16). In our study, approximately 2/3 of the patients had typical and indeterminate COVID-19 chest CT presentation and atypical chest CT presentation was detected in 17.7% of the patients (Figure 4,5).

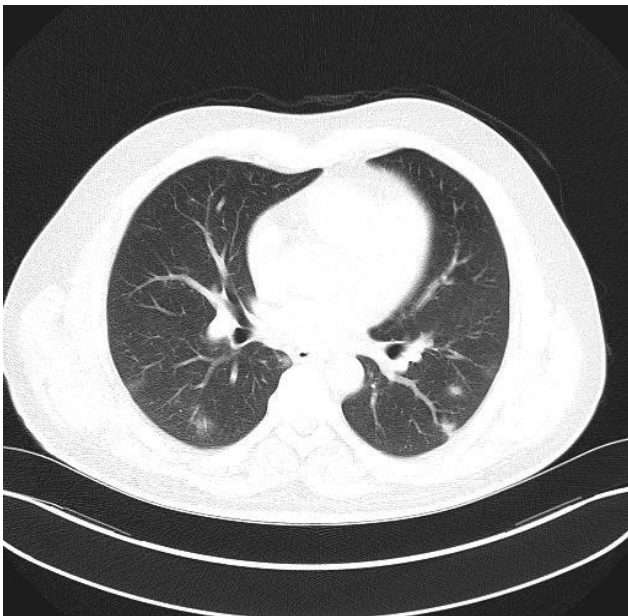


Figure 4. Unenhanced axial image of lungs of in a patient with positive RT-PCR show bilateral peripheral multifocal nodules with surrounding GGO. GGO; ground glass opacity

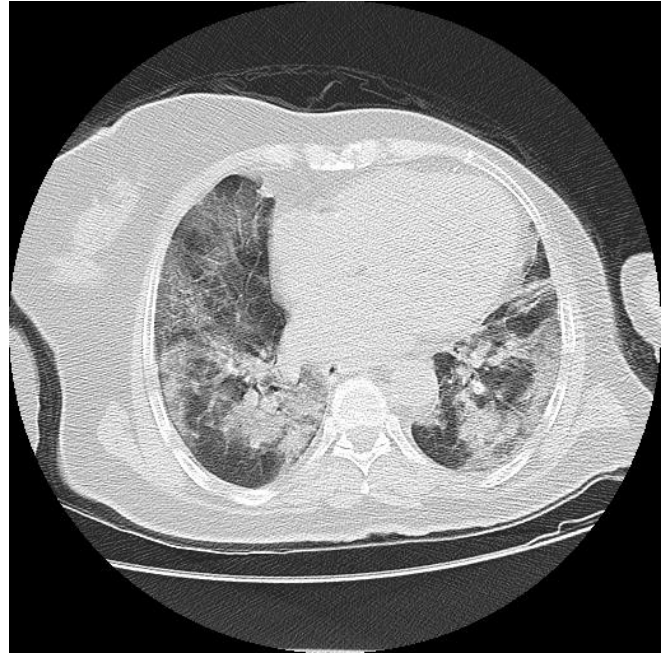


Figure 5. Unenhanced axial image of lungs of in a patient with positive RT-PCR show bilateral, peripheral, posterior diffuse GGO and consolidation. GGO; ground glass opacity

GGO are the earliest findings of the disease which are seen in most of the COVID-19 patients in different studies (17,18). Other early-stage findings are air space consolidations and bronchovascular thickening. Consolidation can sometimes be seen superimposed on ground-glass opacities at the early stages of the disease. Consolidation in COVID-19 pneumonia often lies in segmental style and/or along bronchovascular structures scattered across subpleural regions. As the disease progresses, the density of the consolidation areas, especially in the GGO, and tendencies of consolidation increase and progress to the upper parts of the lungs (19,20). Ground glass density, consolidation, and thickening of the interlobular septum are defined as exudation of the alveoli, filling of the alveoli with inflammatory exudation, and inflammatory involvement of the pulmonary interstitium, respectively (21,22). As expected, in most patients with these findings, high CRP values may be detected at hospital admissions, and CRP increases as the extent of lung findings increases. As the of these Chest CT findings progresses CRP also increases. In our study, as chest CT findings changes from mild to severe according to the BSTI classification, the CRP values increased with statistical significance. There were significant correlations among the degree of pulmonary inflammation and the main clinical symptoms and the laboratory results in patients with classic chest CT findings.

COVID-19 patients may present with less common CT findings such as nodule other than classic CT findings (23). Despite the confusion in defining of discrete nodule or solid nodule, commonly known definition for is as follows: a rounded or irregular opacity with well or poor defined edges, measuring less than 3 cm in diameter (21). Pseudonodular consolidation suggesting a pattern of organizing pneumonia, seen in approximately 10% of

COVID-19 patients, has also been classified as nodular involvement in recent articles (24). Nodule may occur as multifocal, solid irregular or with visible halo in a small number of COVID-19 patients (25,26,27). Multifocal, irregularly bounded nodules with minimal ground glass patterns can be seen in 3–13% of cases with COVID-19 pneumonia (26,27). This finding is also observed in other viral pneumonias as similar to COVID-19 (28). Although the underlying pathophysiological mechanism has not been fully elucidated, it is one of the radiological findings of the pulmonary inflammation process of viral pneumonia. The relationship between pulmonary inflammation which is one of the main predictors of mortality in COVID-19 patients and inflammatory marker CRP was shown (29). But it is not exactly known what kind of relationship exists between different type of chest CT parenchymal findings which are radiological markers of pulmonary inflammation and CRP. On this basis, we aimed to investigate the relation between chest CT findings such as distribution and severity of pulmonary involvement and CRP. It was not surprising to us to find that CRP value increased significantly in parallel to the severity of the lung involvement defined according to BSLI. Additionally it was found that COVID-19 patients with presence of nodule presentation had statistically significant lower CRP values compared to the patients with typical presentation on chest CT at hospital admission. The studies investigating the relationship between Chest CT and CRP in COVID-19 patients have found a correlation between the severity of pneumonia and CRP (29-31). These results were also consistent with our study. The main limitations of these studies were inclusion of small-number populations, use of different methods to determine the severity of pulmonary involvement, and poor statistical analysis. However, the relationship of chest CT findings such as GGO, crazy paving, and nodule with CRP value has not been evaluated previously and there are no studies in the literature investigating this association in COVID-19 patients. Our study differs from other studies in this aspect since it is the first study that investigated this association.

CONCLUSION

Chest CT is used in diagnosis and follow-up of COVID-19 patients. The relationship between the typical findings and their distribution is known with inflammation markers and this relationship plays an important role in the hospitalization and clinical follow-up of COVID-19 patients. There are insufficient data to make a similar interpretation in patients with atypical chest CT presentations. In our study, we found that patients with atypical findings as nodules had lower CRP levels than those with typical findings on chest CT in symptomatic COVID-19 patients admitted to the hospital. It may require for further studies to assess whether this finding has clinical implication.

Limitations

The main limitation of the study was the discrepancy in the definition of the nodule observed on

chest CT. Another important limitation was the lack of chest CT follow-ups, so the progression of the nodules detected at presentation cannot be tracked down. In addition, clinical implication of atypical chest CT presentation such as node was not evaluated.

Ethics Committee Approval: Gazi Yaşargil E.A.H 537/24.07.2020

Conflict of Interest: There is no conflict of interest.

Funding: There is no financial support.

Informed Consent: This a retrospective study.

REFERENCES

1. Shah A, Kashyap R, Tosh P, Sampathkumar P, O'Horo JC. Guide to Understanding the 2019 Novel Coronavirus. *Mayo Clin Proc.* 2020; Apr;95(4):646-652 <https://doi.org/10.1016/j.mayocp.2020.02.003>.
2. Mahase E. Covid-19: WHO declares pandemic because of "alarming levels" of spread, severity, and in action. *BMJ.* 2020;368:m1036. doi: 10.1136/bmj.m1036.
3. Lippi G, Sanchis-Gomar F, Henry BM. Coronavirus disease 2019 (COVID-19): the portrait of a perfect storm. *AnnTranslMed* 2020; 2020 Apr;8(7):497.doi: 10.21037/atm.2020.03.157.
4. Ai T, Yang Z, Hou H, Zhan C, Chen C, Lv W, et al. Correlation of chest CT and RTPCR testing in coronavirus disease 2019 (COVID-19) in China: a report of 1014 cases. *Radiology.* 2020 Aug;296(2):E32-E40.doi: 10.1148/radiol.2020200642.
5. Fang Y, Zhang H, Xie J, Lin M, Ying L, Pang P, et al. Sensitivity of chest CT for COVID-19: comparison to RT-PCR. *Radiology* 2020 Aug;296(2):E115-E117.doi: 10.1148/radiol.2020200432.
6. Revel M-P, Parkar AP, Prosch H, Silva M, Sverzellati M, Gleeson F, et al. COVID-19 patients and the radiology department—advice from the European Society of Radiology (ESR) and the European Society of Thoracic Imaging (ESTI). *EurRadiol.* 2020 Sep;30(9):4903-4909.doi: 10.1007/s00330-020-06865-y.
7. Pan F, Ye T, Sun P, Gui S, Liang B, Li L, et al. Time course of lung changes at chest CT during recovery from coronavirus disease 2019 (COVID-19). 2020 Jun;295(3):715-721. doi: 10.1148/radiol.2020200370.
8. Hani C, Trieu NH, Saab I, Dangeard S, Bennani S, Chassagnon G, et al. COVID-19 pneumonia: a review of typical CT findings and differential diagnosis. *Diagn Interv Imagin* 2020 May;101(5):263-268.doi: 10.1016/j.diii.2020.03.014.
9. Wen Z, Chi Y, Zhang L, Liu H, Du K, Li Z, et al. Coronavirus disease 2019: initial detection on chest CT in a retrospective Multicenter study of 103 chinese subjects. *Radiology:Cardiothoracic Imaging* 2020; 200092. doi.org/10.1148/ryct.2020200092.
10. Inui S, Fujikawa A, Jitsu M, Kunishima N, Watanabe S, Suzuki Y, et al. Chest CT findings in cases from the cruise ship "Diamond Princess" with coronavirus disease 2019 (COVID-19). *Radiology Cardiothoracic Imaging.* 2020; 200110.doi.org/10.1148/ryct.2020200110

11. Fang Y, Zhang H, Xie J, Lin M, Ying L, Pang Pet al. Sensitivity of chest CT for COVID19: Comparison to RT-PCR. *Radiology*. 2020 Aug;296(2):E115-E117.doi: 10.1148/radiol.2020200432.
12. World Medical Association Declaration of Helsinki: ethical principles for medical research involving human subjects. *JAMA* 2000; 284:3043–3049
13. Ding X, Xu J, Zhou J, Long Q. Chest CT findings of COVID-19 pneumonia by duration of symptoms . *Eur J Radiol*. 2020 Jun;127:109009. doi: 10.1016/j.ejrad.2020.109009
14. Ye Z, Zhang Y, Wang Y, Huang Z, Song B. Chest CT manifestations of new coronavirus disease 2019 (COVID-19): a pictorial review. *Eur Radiol*. 2020 Aug;30(8):4381-4389. doi: 10.1007/s00330-020-06801-0.
15. Simpson S, Kay FU, Abbara S, Bhalla S, Chung JH, Chung M, et al. Radiological Society of North America Expert Consensus Statement on Reporting Chest Ct Findings Related to COVID-19. Endorsed by the Society of Thoracic Radiology, The American College of Radiology and RSNA-Secondary Publication. *J Thorac Imaging*. 2020 Jul;35(4):219-227. doi: 10.1097/RTI.0000000000000524
16. BSTI. Thoracic imaging in COVID-19 infection. Guidance for the Reporting Radiologist British Society of thoracic imaging. Available at https://www.bsti.org.uk/media/resources/files/BSTI_COVID_19_Radiology_Guidance_version_2_16.03.20.pdf. [Accessed 13 April 2020]
17. Song FX, Shi NN, Zhang ZY, Shen J, Lu H, Ling Y, et al. Emerging coronavirus 2019-nCoV pneumonia. *Radiology*. 2020;200274. doi.org/10.1148/radiol.2020200274
18. Duan YN, Qin J. Pre- and posttreatment chest CT findings: 2019 novel coronavirus (2019-ncov) pneumonia. *Radiology*. 2020;200323. doi:10.1148/ radiol.2020200323.
19. Pan F, Yan TH, Sun P, Gui S, Liang B, Li L, et al. Time course of lung changes on Chest CT during recovery from 2019 novel coronavirus (COVID-19) pneumonia. *Radiology*. 2020;200370. doi:10.1148/radiol.2020200370
20. Jeffrey K. Chest CT findings in 2019 novel coronavirus (2019-nCoV) infections from Wuhan, China: key points for the radiologist. *Radiology*. 2020;200241. doi:10.1148/radiol.202020024
21. Hansell DM, Bankier AA, MacMahon H, McLoud TC, Muller NL, Remy J (2008) Fleischner Society: glossary of terms for thoracic imaging. *Radiology*. 2008 Mar;246(3):697-722. doi: 10.1148/radiol.2462070712.
22. Shi H, Han X, Jiang N, Cao Y, Alwalid O, Gu J, et al. Radiological findings from 81 patients with COVID-19 pneumonia in Wuhan, China: a descriptive study. *Lancet Infect Dis*. 2020 Apr;20(4):425-434.doi: 10.1016/S1473-3099(20)30086-4.
23. Bernheim A, Mei X, Huang M, Yang Y, Fayad ZA, Zhang N et al. Chest CT findings in coronavirus disease-19 (COVID-19): relationship to duration of infection. *Radiology* 2020;295:200463. Doi: 10.1148/radiol.2020200463
24. Bekci T. “Reversed halo sign” on 3D CT in COVID-19. *Diagn Interv Radiol*. 2020 Jul;26(4):379.doi: 10.5152/dir.2020.20254.
25. Pan Y, Guan H, Zhou S, Wang Y, Li Q, Zhu T et al. Initial CT findings and temporal changes in patients with the novel coronavirus pneumonia (2019- nCoV): a study of 63 patients in Wuhan, China. *EurRadiol*. 2020 Jun;30(6):3306-3309.doi: 10.1007/s00330-020-06731-x
26. Ai T, Yang Z, Hou H Zhan C, Chen C, Lv W, et al. Correlation of chest CT and RTPCR testing in coronavirus disease 2019 (COVID-19) in China: a report of 1014 cases. *Radiology*. 2020 Aug;296(2):E32-E40. doi: 10.1148/radiol.2020200642.
27. Li X, Zeng X, Liu B, Yu Y. COVID-19 infection presenting with CT halosign. *Radiology: Cardiothoracic Imaging* 2020; 200026. doi.org/10.1148/ryct.2020200026
28. Franquet T. Imaging of pulmonary viral pneumonia. *Radiology*. 2011 Jul;260(1):18-39.doi: 10.1148/radiol.11092149.
29. Wu J, Wu X, Zeng W, Guo D, Fang Z, Chen L, et al. Chest CT Findings in Patients With Coronavirus Disease 2019 and Its Relationship With Clinical Features. *Invest Radiol*. 2020 May;55(5):257-261. doi: 10.1097/RLI.0000000000000670.
30. Xiong Y, Sun D, Liu Y, Fan Y, Zhao L, Li X, et al. Clinical and high-resolution CT features of the COVID-19 Infection: Comparison of the initial and follow-up changes. *Invest Radiol*. 2020 Jun;55(6):332-339. doi: 10.1097/RLI.0000000000000674
31. Chen W, Zheng KI, Liu S, Yan Z, Xu C, Qiao Z. Plasma CRP level is positively associated with the severity of COVID-19. *Ann Clin Microbiol Antimicrob*. 2020 May 15;19(1):18. doi: 10.1186/s12941-020-00362-2.e clinical and laboratory presentations of primary and secondary glomerular diseases. *Ren Fail*. 2011;33(8):781-4.
34. Bray C, Bell LN, Liang H, Haykal R, Kaikow F, Mazza JJ, et al. Erythrocyte Sedimentation Rate and C-reactive Protein Measurements and Their Relevance in Clinical Medicine. *WMJ*. 2016;115(6):317-21.
35. Neale TJ, Ojha PP, Exner M, Poczewski H, Ruger B, Witzum JL, et al. Proteinuria in passive Heymann nephritis is associated with lipid peroxidation and formation of adducts on type IV collagen. *J Clin Invest*. 1994;94(4):1577-84.
36. O'Donnell MP, Kasiske BL, Kim Y, Atluru D, Keane WF. Lovastatin inhibits proliferation of rat mesangial cells. *J Clin Invest*. 1993;91(1):83-7.
37. Takemura T, Yoshioka K, Aya N, Murakami K, Matumoto A, Itakura H, et al. Apolipoproteins and lipoprotein receptors in glomeruli in human kidney diseases. *Kidney Int*. 1993;43(4):918-27.
38. Keane WF, O'Donnell MP, Kasiske BL, Kim Y. Oxidative modification of low-density lipoproteins by mesangial cells. *J Am Soc Nephrol*. 1993;4(2):187-94.
39. Gupta S, Rifici V, Crowley S, Brownlee M, Shan Z, Schlondorff D. Interactions of LDL and modified LDL with mesangial cells and matrix. *Kidney Int*. 1992;41(5):1161-9.
40. Oda H, Keane WF. Recent advances in statins and the kidney. *Kidney Int Suppl*. 1999;71:S2-5.
41. Galle J, Heermeier K. Angiotensin II and oxidized LDL: an unholy alliance creating oxidative stress. *Nephrol Dial Transplant*. 1999;14(11):2585-9.
42. Bianchi S, Bigazzi R, Caiazza A, Campese VM. A controlled, prospective study of the effects of atorvastatin on

proteinuria and progression of kidney disease. *Am J Kidney Dis.* 2003;41(3):565-70.

43.Hunsicker LG, Adler S, Caggiula A, England BK, Greene T, Kusek JW, et al. Predictors of the progression of renal disease in the Modification of Diet in Renal Disease Study. *Kidney Int.* 1997;51(6):1908-19.

44.Ruggenti P, Perna A, Tonelli M, Loriga G, Motterlini N, Rubis N, et al. Effects of add-on fluvastatin therapy in patients with chronic proteinuric nephropathy on dual renin-angiotensin system blockade: the ESPLANADE trial. *Clin J Am Soc Nephrol.* 2010;5(11):1928-38.

https://doi.org/10.4103/ijem.IJEM_183_18